EPJ manuscript No.
(will be inserted by the editor)

Output Stream of single inhibitory neuron with delayed feedback. Fast Cl-type inhibition

Alexander K. Vidybida and Kseniya G. Kravchuk

Bogolyubov Institute for Theoretical Physics, Metrologichna str. 14-B, 03680 Kyiv, Ukraine e-mail: vidybida@bitp.kiev.ua

Received: date / Revised version: date

Abstract. A single inhibitory neuron with delayed feedback is considered. The neuron receives an excitatory input from the Poisson stream, and inhibitory impulses from the feedback line with delay. We investigate here, how does the feedback presence affect the output firing statistics of inhibitory neuron. Using binding neuron (BN) as a model, we derive exact analytical expressions for the output interspike intervals (ISI) probability density, mean output ISI and coefficient of variation as functions of model's parameters for the case of threshold 2. Using leaky integrate-and-fire (LIF) model, as well as BN model with higher thresholds, these statistical quantities are found numerically. In contrast to the previously studied situation of no feedback, the ISI probability densities found here both for BN and LIF neuron become bimodal and have discontinuity of jump type. Nevertheless, the delayed feedback presence was not found to affect substantially the output ISI coefficient of variation. The ISI coefficient of variation found ranges between 0.5 and 1. It is concluded that introduction of delayed feedback can radically change neuronal output firing statistics of inhibitory neuron. This statistics is as well distinct of what was found previously for excitatory neuron with delayed feedback.

PACS. 87.19.ll Models of single neurons and networks – 87.10.-e General theory and mathematical aspects – 87.10.Ca Analytical theories – 87.10.Mn Stochastic modeling

1 Introduction

A realistic neuronal network is normally characterized with a complicated system of excitatory and inhibitory interconnections between individual neurons the network is composed of. Statistics of spiking activity of individual neurons can be measured experimentally [7,10,13]. It would be interesting to understand how the details of network's construction might influence statistics of neuronal activity, when the network is driven with some stimulation, or allowed to reverberate freely. Exact theoretical analysis of this question in a developed network represents fair mathematical difficulties.

At the same time, in a real neural network, constructing elements can be found, which allow exact mathematical treatment. The results of such a treatment can shed light on the nature of transformations the neuronal activity might undergo while spreading within a real neural network. One example is an excitatory neuron which sends its output impulses onto its own dendritic tree. This type of constructive element has been found in the olfactory bulb [1,8]. Theoretical study of this construction fed with Poisson stream revealed interesting peculiarities in its output activity statistics [20]. Another natural variant of this construction is an inhibitory neuron with feedback. It seems that selfinhibition happens more frequently in the brain, than selfexcitation. Selfinhibition can be slow, due to potassium channels opening [3], or fast, due to chlorine channels [2, 9]. It also can be direct (through autapses) [2,8,12], or acting through a single intermediate neuron [9]. Also, it can be evoked not only by means of spike delivered to corresponding synaptic connection, but also through extended diffusion of some usual [12], or unusual [3] mediator.

In this paper, we consider situation of inhibitory neuron fed externally with excitatory impulses from Poisson stream of intensity λ, which sends its output impulses to its own input through feedback line with delay time Δ. The inhibition mechanism is fast in a sense, that it cancels excitatory impulses, which neuron obtained recently, and has no any effect on the neuron in its resting state.

For analytical derivation, we take binding neuron (BN) as a neuronal model, see Sec. 2.1 for BN definition. In Secs. 3–6, we derive exact analytical expressions for the output ISI probability density, mean output ISI and coefficient of variation as functions of λ, Δ and BN's internal memory, τ, for BN with threshold 2. In Sec. 7, these statistical quantities are found numerically by means of Monte-Carlo simulations for leaky integrate-and-fire (LIF) model, as well as for BN model with higher thresholds. In contrast to the previously studied situation of neuron without feedback, and of excitatory neuron with delayed feedback, the ISI probability densities found here both for excitatory BN and excitatory LIF neuron are bimodal. Also they retain discontinuity of jump type obsereved before for the excitatory neuron with feedback. In the case of instantaneous ($\Delta = 0$) feedback, as it could be expected namely for fast shunt-

ing inhibition, the feedback line has no effect on the output activity of inhibitory neuron.

2 Object definition

2.1 BN without feedback

The binding neuron model [16] is inspired by numerical simulation [15] of Hodgkin-Huxley-type point neuron, as well as by the leaky integrate-and-fire (LIF) model [11]. In the binding neuron, the trace of an input is remembered for a fixed period of time after which it disappears completely. This is in the contrast with the above two models, where the postsynaptic potentials decay exponentially and can be forgotten only after triggering. The finiteness of memory in the binding neuron allows one to construct fast recurrent networks for computer modeling as well as obtain exact mathematical conclusions concerning firing statistics of BN. Recently, the finiteness is utilized for exact mathematical description of the output stochastic process if the binding neuron is driven with the Poisson input stream in the case of no feedback [18], for BN with instantaneous feedback [19] and for excitatory BN with delayed feedback [20].

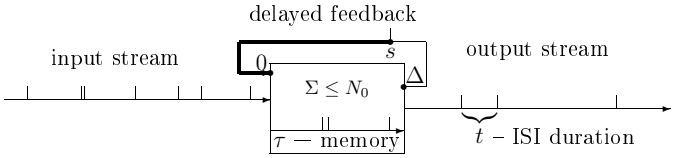

Fig. 1. Binding neuron with feedback (see [16] for deatils). τ is similar to the "tolerance interval" discussed in [6, p. 42]. Multiple input lines with Poisson streams are joined into a single one here.

The BN works as follows (see Fig. 1 with the feedback line removed). All excitatory input impulses have the same magnitude. Each one of them is stored in the BN for a fixed period of time, τ, and then is forgotten. When the number of stored excitatory impulses, Σ, becomes equal to the BN's threshold, N_0, the BN fires output spike, clears its internal memory, and is ready to receive fresh inputs. Thus, the state just after firing corresponds to the resting state of excitable membrane in real neurons, and presence of impulses in the internal memory of BN corresponds to partially depolarised state. In this work, we take BN with $N_0 = 2$ for analytical derivation. BNs with higher thresholds are studied numerically in Sec. 7.

Normally, any neuron has a number of input lines. If input stream in each line is Poissonian and all lines have the same weight, all of them can be joined into a single one, like in Fig. 1, with intensity, λ, equal to sum of intensities in the individual lines.

The output statistics for BN without feedback was calculated if $N_0 = 2$ (see [18] for details). ISI probability density function, $P^0(t)$, where $t > 0$ denotes the output ISI duration, was obtained as

$$m\tau \le t \le (m+1)\tau \quad \Rightarrow \quad P^0(t) = y_m(t), \quad m = 0,1,\ldots, \quad (1)$$

where $y_i(t)$ are defined according to the following recurrent relation:

$$y_i(t) = y_{i-1}(t) + \frac{\lambda^{i+2}}{(i+1)!}\,(t-i\tau)^{i+1}e^{-\lambda t} - \frac{\lambda^{i+1}}{i!}\,(t-i\tau)^{i}e^{-\lambda t},$$
$$y_0(t) = e^{-\lambda t}\lambda^2\, t, \quad i = 0,1,\ldots, \quad t > 0. \quad (2)$$

$P^0(t)$ is a unimodal function, which reaches its maximum at $\min(\frac{1}{\lambda};\tau)$. Example of $P^0(t)$ is given in Fig. 9, left.

The first moment, W_1^0, of the probability density (1) was found as

$$W_1^0 \equiv \int_0^\infty t\,P^0(t)\,dt = \frac{1}{\lambda}\left(2 + \frac{1}{e^{\lambda\tau}-1}\right), \quad (3)$$

which will be used later.

In this work, we also utilize the probability $\Pi(t)$ to get an output ISI, which is longer than t:

$$\Pi(t) \equiv \int_t^\infty P^0(t)\,dt. \quad (4)$$

The exact expression for $\Pi(t)$ for an arbitrary t, which is cumbersome, can be found in [17]. We will need the expression for $\Pi(t)$ only at the domain $t < \tau$, where it reduces to the following

$$\Pi(t) = (1+\lambda t)\,e^{-\lambda t}, \qquad t < \tau. \quad (5)$$

2.2 Feedback line action

In this work, we consider the situation, when BN receives excitatory input from the Poisson stream and inhibitory impulses from the feedback line.

We assume, that time delay Δ of impulse in the feedback line is smaller than the BN's memory duration, τ:

$$\Delta < \tau. \quad (6)$$

It allows to make analytical expressions shorter. Also, the assumption (6) is consistent with the case of direct feedback, not mediated by other neurons.

If the line is empty, when neuron fires, an output impulse enters the line and after delay Δ reaches neuron's input. If the line already keeps an impulse at the moments of BN firing, it does not accept the new one. It means, that at any given moment, the feedback line either keeps one impulse, or conveys no impulses, and cannot convey two or more impulses at the same time. If so, the state of the feedback line can be described with a single variable. For this purpose, we introduce the stochastic variable s, $s \in]0;\Delta]$, which gives the time to live of the impulse in the feedback line, see Fig 1. Hereinafter, we will use the values of s just at the moments of output ISI beginings (just after BN firings).

The inhibitory action of feedback impulses is modelled in the following way. When the inhibitory impulse reaches BN, it annihilates all excitatory impulses already present in BN's memory, similarly as *Cl*-type inhibition shunts depolarization of excitable membrane. If at the moment of inhibitory impulse arrival, the BN is empty, then the impulse desappears without any action, similarly as *Cl*-type inhibition does not affect membrane's voltage in its resting state. Such inhibition is "fast" in that sense, that the inhibitory impulses act instantaneously and are not remembered by neuron.

3 Derivation outline

It is clear, that both the binding neuron and the feedback line operate in deterministic manner. Nevertheless, the probabilistic description is required for the output stream because of the stochastic nature of driving Poisson process.

Let us denote by $P^{\Delta}(t)$ the ISI probability density function for inhibitory neuron with delayed feedback. In order to calculate $P^{\Delta}(t)$, we use the procedure, previously utilized for excitatory BN with delayed feedback [20]. As a first step, we define the conditional probability density, $P^{\Delta}(t \mid s)$. Namely, $P^{\Delta}(t \mid s)$ gives the probability to obtain an output ISI of duration within interval $[t; t+dt[$, provided there was an impulse in the feedback line with time to live equal s at the moment of this ISI begining.

Then, we introduce the stationary probability density, $f(s)$, for time to live, $s \in]0;\Delta]$, of an impulse in the feedback line at the moment of beginning of any output ISI.

The output ISI probability density can be calculated based on the expressions for $P^{\Delta}(t \mid s)$ and $f(s)$, namely:

$$P^{\Delta}(t) = \int_0^{\Delta} P^{\Delta}(t \mid s) f(s)\, ds. \tag{7}$$

In order to find $f(s)$, we first obtain the transition probability density $P(s' \mid s)$, $s, s' \in]0;\Delta]$, which gives the probability that at the begining of some output ISI, the line has impulse with time to live within interval $[s'; s'+ds'[$, provided that at the beginning of the previous ISI it had impulse with time to live equal s. $f(s)$ is then found as normalized to 1 solution of the following equation:

$$\int_0^{\Delta} P(s' \mid s)\, f(s)\, ds = f(s'). \tag{8}$$

In the next section, we are going to find explicit expressions for probability densities $P^{\Delta}(t \mid s)$, $P(s' \mid s)$ and $f(s)$.

4 Main calculation

4.1 Conditional probability density $P^{\Delta}(t \mid s)$

In order to derive $P^{\Delta}(t \mid s)$, domains $t < s$ and $t \geq s$ should be considered separately.

In the case $t < s$, the output impulse must be generated without the line impulse involved. Therefore, probability density for such ISI values is the same as for BN without any feedback:

$$P^{\Delta}(t \mid s) = P^0(t), \quad t < s. \tag{9}$$

Here $P^0(t)$ is the output ISI probability density for BN without feedback, given in Eq. (1).

At the moment s, the inhibitory feedback impulse reaches BN and BN becomes empty. As it is impossible to obtain more than one impulse from the Poisson stream within infinitesimally small time interval $[s; s+dt[$, $P^{\Delta}(t \mid s) = 0$ when $t = s$.

In order to obtain ISI $t > s$, two independent events must occure: (i) BN without feedback fires no spikes during time interval $]0;s]$; (ii) BN without feedback starts emty at moment s and is firstly triggered at moment t. These events are independent since their realizations are defined by behavior of Poisson input stream on disjoint intervals $]0;s]$ and $]s;t]$. By definition of $\Pi(t)$, see Eq. (4), the probability to have (i) is $\Pi(s)$, and (ii) has the probability $P^0(t-s)\,dt$. Therefore,

$$P^{\Delta}(t \mid s) = \Pi(s)\, P^0(t-s), \quad t > s. \tag{10}$$

The conditional probability density $P^{\Delta}(t \mid s)$, given in (9) and (10), is normalized: $\int_0^{\infty} P^{\Delta}(t \mid s)\, dt = 1$.

Taking into account Eq. (5), (9) and (10) for the case $\Delta < \tau$ one obtains $P^{\Delta}(t \mid s)$ as follows:

$$P^{\Delta}(t \mid s) = \begin{cases} \lambda^2 t\, e^{-\lambda t}, & t \in]0;s[, \\ (1+\lambda s)\, e^{-\lambda s} P^0(t-s), & t \geq s. \end{cases} \tag{11}$$

$P^{\Delta}(t \mid s)$, given in (11), has a break of height $\lambda^2 s\, e^{-\lambda s}$ at $t = s$.

4.2 Transition probability density $P(s' \mid s)$

From the meaning of $P^{\Delta}(t \mid s)$ it follows that Eq. (9) allows to calculate $P(s' \mid s)$ for $s' < s$, namely:

$$P(s' \mid s) = P^{\Delta}(s - s' | s) = P^0(s - s'), \quad s' < s \in]0;\Delta]. \tag{12}$$

As the feedback line conveys no more than one impulse at any given moment, it is impossible to have $s < s' < \Delta$. Therefore,

$$P(s' \mid s) = 0, \quad s < s' < \Delta. \tag{13}$$

Consider the exact equality $s' = \Delta$. It is realized every time, when for previous ISI $t \geq s$, and this inequality happens with non-zero probability. Therefore, the probability density $P(s' \mid s)$ has singularity of δ-function type at $s' = \Delta$. For calculating its mass, one should obtain the probability of $t \geq s$ by integrating Eq. (10) over suitable values of t:

$$\begin{aligned} P(s' \mid s) &= \delta(s' - \Delta) \int_s^{\infty} dt\; P^{\Delta}(t \mid s) = \\ &= \delta(s' - \Delta) \cdot \Pi(s) \int_s^{\infty} P^0(t-s)\, dt = \\ &= \Pi(s)\, \delta(s' - \Delta), \quad s' \geq s \in]0;\Delta]. \end{aligned} \tag{14}$$

Here we use $\int_0^{\infty} P^0(t)\, dt = 1$.

The transition probability density $P(s' \mid s)$, given in Eqs. (12) – (14) is normalized: $\int_0^{\Delta} P(s' \mid s)\, ds' = 1$.

Note, that Eqs. (12) and (14) could be obtained directly, without refering to $P^{\Delta}(t \mid s)$. Indeed, if $s' < s$, then the ISI $t = s - s'$ was obtained without feedback line envolved. Therefore, $P(s' \mid s)$ is determined by probability to obtain ISI of duration t from BN without feedback, which gives (12).

The exact equality $s' = \Delta$ is realized when BN without feedback fires no spikes at $]0;s]$. The probability of this event is $\Pi(s)$, which gives (14) for conditional probability density.

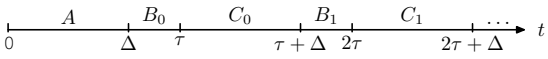

Fig. 2. Domains of t used for calculating integral in (19).

Substituting $P^0(s-s')$ from (1) and $\Pi(s)$ from (5), one obtains $P(s' \mid s)$ for the case $\Delta < \tau$ in the following form:

$$P(s' \mid s) = \begin{cases} e^{-\lambda(s-s')}\lambda^2(s-s'), & s > s' \in]0;\Delta], \\ (\lambda s+1)\, e^{-\lambda s}\, \delta(s'-\Delta), & s' \geq s. \end{cases} \qquad (15)$$

Interestingly, that obtained expressions for $P(s' \mid s)$ are the same, as those, previously found for excitatory BN with delayed feedback [20].

4.3 Delays probability density

In order to find $f(s)$, one should substitute $P(s' \mid s)$ from (15) into (8) and solve the obtained equation. As $P(s' \mid s)$ obtained is exactly the same as for excitatory BN with delayed feedback [20], the equation for $f(s)$ and $f(s)$ itself will also be the same. In [20], the probability density $f(s)$ was obtained as

$$f(s) = a\,\delta(s-\Delta) + g(s), \qquad (16)$$

where $g(s)$ – is an ordinary function, which vanishes out of interval $]0;\Delta]$:

$$g(s) = \frac{a\lambda}{2}\left(1 - e^{-2\lambda(\Delta-s)}\right), \quad s \in]0;\Delta], \qquad (17)$$

and a – is a dimensionless constant:

$$a = \frac{4e^{2\lambda\Delta}}{(2\lambda\Delta+3)e^{2\lambda\Delta}+1}, \qquad (18)$$

which gives the probability to find the impulse in the feedback line with time to live Δ at the beginning of arbitrary ISI.

5 ISI probability density

In order to find $P^\Delta(t)$, one should substitute (11) and (16) into Eq. (7), which gives:

$$P^\Delta(t) = aP^\Delta(t \mid \Delta) + \int_0^\Delta P^\Delta(t \mid s)g(s)ds. \qquad (19)$$

As the explicit expressions for $P^\Delta(t \mid s)$ are different for different domains of t (see Eqs. (11) and (1)), further transformation of (19) depends on the domain, the t belongs to. The first few domains of t are shown in Fig. 2.

Consider case A, where $t \in]0;\Delta[$. Here integration domain in (19) should be splitted into two with point $s = t$, see both top and bottom line of Eq. (11). This gives

$$P^\Delta(t) = \int_0^t (1+\lambda s)\, e^{-\lambda s}\lambda^2(t-s)e^{-\lambda(t-s)}\, g(s)\, ds + \\ + \int_t^\Delta \lambda^2 t e^{-\lambda t} g(s)\, ds + a\,\lambda^2 t\, e^{-\lambda t},$$

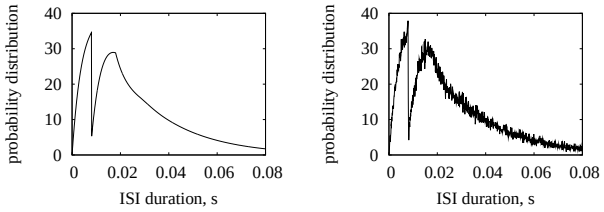

Fig. 3. Example of ISI probability density function, calculated in accordance with Eqs. (20), (23), (24), *left*, and numerically, by means of Monte Carlo method, *right*. For both panels: $\tau = 10$ ms, $\Delta = 8$ ms, $\lambda = 10$ s^{-1}, $N_0 = 2$. Curve found numerically fits perfectly with one shown in the left panel. In the numerical experiment 10^5 spikes were produced.

which after transformations becomes

$$P^\Delta(t) = \frac{2\lambda\, e^{-\lambda t}}{2\lambda\Delta+3+e^{-2\lambda\Delta}} \cdot \left(\frac{1}{6}\lambda^3 t^3 - \frac{1}{2}\lambda^2 t^2 + \right. \\ \left. + \lambda t\left(\frac{3}{2} + \frac{1}{4}e^{-2\lambda\Delta} + \frac{1}{4}e^{-2\lambda(\Delta-t)}\right) + \lambda^2 t\Delta \right), \quad t < \Delta. \qquad (20)$$

When $t \geq \Delta$, one needs only the bottom line of Eq. (11) to calculate $P^\Delta(t)$, and Eq. (19) turns into the following:

$$P^\Delta(t) = a(1+\lambda\Delta)\, e^{-\lambda\Delta}P^0(t-\Delta) + \\ + \int_0^\Delta (1+\lambda s)\, e^{-\lambda s}P^0(t-s)g(s)\, ds.$$

Let us introduce a new variable of integration, $u = t - s$:

$$P^\Delta(t) = a(1+\lambda\Delta)\, e^{-\lambda\Delta}P^0(t-\Delta) + \\ + \int_{t-\Delta}^t (1+\lambda(t-u))e^{-\lambda(t-u)}P^0(u)g(t-u)\, du. \qquad (21)$$

In order to perform integration in (21), we define two groups of domains, B_m and C_m, namely:

$$B_m = [m\tau+\Delta;(m+1)\tau], \qquad m = 0,1,\ldots, \\ C_m =](m+1)\tau;(m+1)\tau+\Delta[, \qquad m = 0,1,\ldots.$$

Note, that the full domain $[\Delta;\infty[$ is completely covered by alternate domains B_m and C_m, $m = 0,1,\ldots$.

If $t \in B_m$, then $m\tau \leq t-\Delta < t \leq (m+1)\tau$, and one should substitute $y_m(t)$ from (2), corresponding to that m, instead of $P^0(u)$ in the (21). If $t \in C_m$, then $m\tau < t-\Delta < (m+1)\tau < t$. Therefore, the domain of integration in the Eq. (21) should be split into subdomains two with point $(m+1)\tau$, and as $P^0(u)$ one should substitute either $y_m(t)$, or $y_{m+1}(t)$ depending on subdomain.

5.1 ISI probability density at the domains B_m

Thus, in the case $t \in B_m$, one obtains for $P^\Delta(t)$:

$$P^\Delta(t) = a(1+\lambda\Delta)\, e^{-\lambda\Delta}y_m(t-\Delta) + \\ + \int_0^\Delta (1+\lambda s)\, e^{-\lambda s}y_m(t-s)g(s)ds, \quad t \in B_m, \qquad (22)$$

which after integration gives:

$$P^{\Delta}(t) = a(1+\lambda\Delta)\,e^{-\lambda\Delta}\cdot y_m(t-\Delta)- -\frac{a}{2}\,e^{\lambda(\Delta-\tau)}\cdot y_{m+1}(t-\Delta+\tau)+\frac{a}{2}\,e^{\lambda\tau}\cdot y_{m+1}(t+\tau)+ +\frac{a\lambda}{2}\,e^{-\lambda t}\sum_{k=1}^{m+1}\sum_{l=0}^{k}K_{kl}\lambda^{k-l}(t-(k-1)\tau)^{k-l}- -\frac{a\lambda}{2}\,e^{-\lambda t}\sum_{k=1}^{m}\sum_{l=0}^{k}K_{kl}\lambda^{k-l}(t-k\tau)^{k-l},\quad t\in B_m, \quad (23)$$

where

$$K_{kl}=\frac{1}{2^{l+2}(k-l)!}\left(\frac{l+1}{(l+2)!}(-2\lambda\Delta)^{l+2}+l+1- -(l-1)e^{-2\lambda\Delta}-2\sum_{i=0}^{l}\frac{(-2\lambda\Delta)^{l-i}}{(l-i)!}\left(1+\frac{l+1}{l+1-i}\cdot\lambda\Delta\right)\right).$$

5.2 ISI probability density at the domains C_m

Consider the case $t\in C_m$. Taking into account Eqs. (1) and (2), one can rewrite (21) as follows

$$P^{\Delta}(t)\Big|_{t\in C_m} = a(1+\lambda\Delta)\,e^{-\lambda\Delta}y_m(t-\Delta)+ +\int_0^{t-(m+1)\tau}(1+\lambda s)\,e^{-\lambda s}y_{m+1}(t-s)g(s)ds+ +\int_{t-(m+1)\tau}^{\Delta}(1+\lambda s)\,e^{-\lambda s}y_m(t-s)g(s)ds=$$

$$=a(1+\lambda\Delta)\,e^{-\lambda\Delta}y_m(t-\Delta)+\int_0^{\Delta}(1+\lambda s)\,e^{-\lambda s}y_m(t-s)g(s)ds+ +\frac{\lambda^{m+3}}{(m+2)!}\,e^{-\lambda t}\int_0^{t-(m+1)\tau}(1+\lambda s)\,(t-s-(m+1)\tau)^{m+2}g(s)ds- -\frac{\lambda^{m+2}}{(m+1)!}\,e^{-\lambda t}\int_0^{t-(m+1)\tau}(1+\lambda s)\,(t-s-(m+1)\tau)^{m+1}g(s)ds.$$

It is useful to denote as $P^{\Delta}_{B,m}(t)$ the righthand side of Eq. (22) defined for all t:

$$P^{\Delta}_{B,m}(t)=a(1+\lambda\Delta)\,e^{-\lambda\Delta}y_m(t-\Delta)+ +\int_0^{\Delta}(1+\lambda s)\,e^{-\lambda s}y_m(t-s)g(s)ds,\quad t>0,$$

With this notation, one obtaines:

$$P^{\Delta}(t)\Big|_{t\in C_m}=P^{\Delta}_{B,m}(t)+\frac{a\lambda}{2}\,e^{-\lambda t}\cdot\rho^{\Delta}_m\left(\lambda\left(t-(m+1)\tau\right)\right), \quad (24)$$

where

$$\rho^{\Delta}_m(x)=\frac{2}{a\lambda}\frac{1}{(m+2)!}\int_0^x(1+v)\,(x-v)^{m+2}g\left(\frac{v}{\lambda}\right)dv- -\frac{2}{a\lambda}\frac{1}{(m+1)!}\int_0^x(1+v)\,(x-v)^{m+1}g\left(\frac{v}{\lambda}\right)dv,\quad m=0,1,\ldots. \quad (25)$$

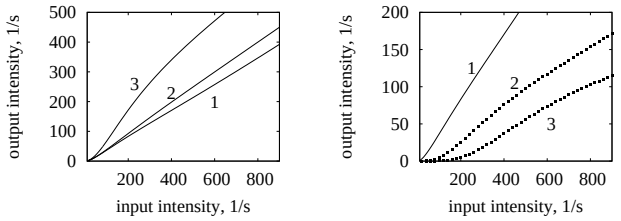

Fig. 4. *Left* – Mean output firing rate as the function of λ for inhibitory BN with delayed feedback (**1**), for BN without feedback [19] (**2**) and for excitatory BN with delayed feedback [20] (**3**), obtained analytically. Curves (**1**)–(**3**): $N_0=2$, τ = 10 ms. $\Delta=2$ ms both for (**1**) and (**3**). *Right* – Mean output firing rate as the function of λ for inhibitory BN with delayed feedback for $N_0=2$ (**1**), obtained analytically, and for $N_0=4$ (**2**) and $N_0=6$ (**3**), found numerically. Curves (**1**)–(**3**): τ = 10 ms, $\Delta=2$ ms, $1\cdot10^6$ triggerings for each point.

Here the dimentionless variable of integration $v=\lambda s$ was introduced.

Performing integration in (25) one obtains:

$$\rho^{\Delta}_m(x)=\sum_{l=0}^{m+4}K_l\,x^l-e^{-2\lambda\Delta+2x}\cdot\sum_{l=0}^{m+3}D_l\,x^l, \quad (26)$$

where

$$K_l=\frac{(m-1-l)}{2^{m+4-l}\cdot l!}\,e^{-2\lambda\Delta},\quad l=0,\ldots m+1;$$

$$K_{m+2}=\frac{1}{4\cdot(m+2)!}\,e^{-2\lambda\Delta}-\frac{1}{(m+2)!};$$

$$K_{m+3}=\sum_{i=1}^{m+2}\frac{(-1)^i\,i}{(m+2-i)!\,(i+1)!}+\frac{1}{(m+3)!};$$

$$K_{m+4}=\sum_{i=0}^{m+2}\frac{(-1)^i\,(i+1)}{(m+2-i)!\,(i+2)!};$$

$$D_l=\frac{1}{2^{m+4-l}}\cdot\sum_{i=0}^{l}\frac{(-1)^{l-i}\cdot(m-1-i)}{i!\,(l-i)!},\quad l=0,\ldots m+1;$$

$$D_{m+2}=\frac{1}{4}\sum_{i=0}^{m+2}\frac{(-1)^i\cdot(i+1)}{i!\,(m+2-i)!};$$

$$D_{m+3}=\frac{1}{2}\sum_{i=0}^{m+2}\frac{(-1)^i}{i!\,(m+2-i)!}. \quad (27)$$

Note, that in the case $\Delta=0$, ISI probability density is completely defined by Eq. (23), which turns into

$$P^{\Delta}(t)|_{\Delta=0}=P^0(t),\quad t>0. \quad (28)$$

This indeed should be the case, because when $\Delta=0$, inhibitory impulses always enter empty neuron and, therefore, the feedback line have no chance to affect the output stream. Naturally, the output ISI distribution for $\Delta=0$ coincides with that found for BN without feedback.

Graph of $P^{\Delta}(t)$ is shown in the Fig. 3.

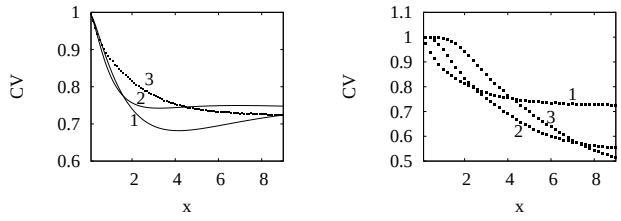

Fig. 5. *Left* – Coefficient of variation vs. $x = \lambda\tau$ for inhibitory BN with delayed feedback for $\Delta = 2$ ms (**1**), $\Delta = 5$ ms (**2**), obtained analytically, and for $\Delta = 20$ ms (**3**), found numerically after 10^6 triggerings for each point. For curves (**1**)–(**3**): $N_0 = 2$, τ = 10 ms. *Right* – Coefficient of variation vs. $x = \lambda\tau$ for inhibitory BN with delayed feedback for $N_0 = 2$ (**1**), $N_0 = 4$ (**2**) and $N_0 = 6$ (**3**), found numerically after 10^6 triggerings for each point. For curves (**1**)–(**3**): τ = 10 ms, $\Delta = 18$.

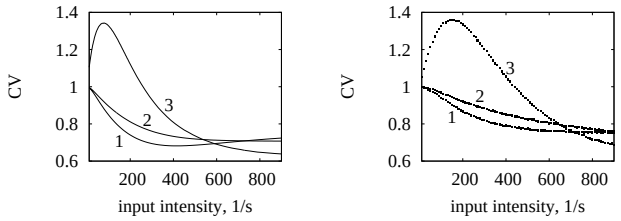

Fig. 6. *Left* – Coefficient of variation vs. λ for inhibitory BN with delayed feedback (**1**), for BN without feedback [19] (**2**) and for excitatory BN with delayed feedback [20] (**3**), obtained analytically. Curves (**1**)–(**3**): $N_0 = 2$, τ = 10 ms. $\Delta = 2$ ms both for (**1**) and (**3**). *Right* – Coefficient of variation vs. λ for inhibitory LIF neuron with delayed feedback (**1**), for LIF neuron without feedback (**2**) and for excitatory LIF neuron with delayed feedback (**3**), found numerically. Curves (**1**)–(**3**): $C = 20$ mV, τ_M = 3 ms, $y_0 = 15$ mV, $1 \cdot 10^6$ triggerings for each point. $\Delta = 2$ ms both for (**1**) and (**3**).

6 Properties of the ISI probability density

6.1 Mean interspike interval

The mean output ISI, W_1^Δ, can be defined as the first moment of the ISI probability density:

$$W_1^\Delta = \int_0^\infty tP^\Delta(t)\,dt.$$

Taking into account Eq. (7), one obtains:

$$W_1^\Delta = \int_0^\infty t\,dt \int_0^\Delta P^\Delta(t\,|\,s)\,f(s)\,ds = \int_0^\Delta ds\,f(s) \int_0^\infty tP^\Delta(t\,|\,s)\,dt,$$

which taken together with Eq. (11) gives:

$$W_1^\Delta = \int_0^\Delta ds\,f(s)\left(\int_0^s t^2 e^{-\lambda t}\lambda^2\,dt + \right.$$
$$\left. + (1+\lambda s)\,e^{-\lambda s} \int_s^\infty tP^0(t-s)\,dt \right) =$$
$$= \frac{1}{\lambda} \int_0^\Delta ds\,f(s)\left(2 + e^{-\lambda s}\left(\lambda W_1^0 - 2 + (\lambda W_1^0 - 1)\,\lambda s\right)\right),$$

where W_1^0 is the mean output ISI for BN without feedback, Eq. (3). Use here (16) and (17), which gives after transformations:

$$W_1^\Delta = a\,(\Delta + W_1^0), \tag{29}$$

where a is given in (18).

Note, that in the case $\Delta = 0$ Eq. (29) turns into the following:

$$W_1^\Delta|_{\Delta=0} = W_1^0,$$

which is consistent with Eq. (28).

Output intensity, λ_o, defined as the mean number of impulses per time unit, is inversed W_1^Δ:

$$\lambda_o^\Delta = \frac{1}{W_1^\Delta} = \frac{(2\lambda\Delta + 3 + e^{-2\lambda\Delta})(1 - e^{-\lambda\tau})}{4(\lambda\Delta + 2 - (\lambda\Delta + 1)e^{-\lambda\tau})} \cdot \lambda, \tag{30}$$

where Eqs. (29), (3) and (18) are used. At large input rates the following relation takes place

$$\lim_{\lambda\to\infty}\left(\frac{\lambda}{2} - \lambda_o^\Delta\right) = \frac{1}{4\Delta}. \tag{31}$$

This limiting relation can be understood as follows. At moderate stimulation some input spikes are lost without influencing output due to high probability of long input ISI. At high intensity every two consecutive excitatory input impulses trigger the BN and send impulse into the feedback line, provided it is empty. Thus, output intensity should be $\lambda/2$ minus firing, inhibited by the line. The maximum rate of ihibitory impulses, which can be delivered by the feedback line to the neuron's input, is $1/\Delta$, and this rate is attaining when $t \to \infty$. Each inhibitory impulse either cancells one excitatory impulse in the neuron, or does nothing, if neuron appears empty at the moment of the feedback line dejection. For high input rates, the probabilities to find neuron empty, or storing one impulse are both approahing 0.5. Thus, due to feedback line activity, about $\frac{1}{2\Delta}$ excitatory impulses will be eliminated from input streem, and about half as much from the output stream, which explaines (31).

Graph of λ_o^Δ is shown at the Fig. 4.

6.2 Coefficient of variation

The coefficient of variation (CV) c_v^Δ of output ISIs is defined as dimentionless dispersion:

$$c_v^\Delta \equiv \sqrt{\frac{W_2^\Delta}{(W_1^\Delta)^2} - 1},$$

where W_2^Δ is the second moment of the ISI probability density:

$$W_2^\Delta \equiv \int_0^\infty t^2\,P^\Delta(t)dt = \int_0^\Delta ds\;f(s) \int_0^\infty t^2\,P^\Delta(t\,|\,s)dt.$$

While calculating W_2^Δ, we use Eq. (3), and finally obtain:

$$(c_v^\Delta)^2 = \frac{B_1\,e^{2\lambda\tau} + 2\,B_2\,e^{\lambda\tau} + B_3}{8\Big((2+\lambda\Delta)\,e^{\lambda\tau} - \lambda\Delta - 1\Big)^2} - 1, \tag{32}$$

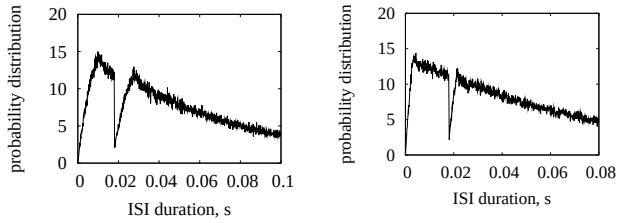

Fig. 7. ISI probability density (measured in s^{-1}), found numerically. *Left* – BN with delayed feedback for $N_0 = 2$, τ = 10 ms, $\Delta = 18$ ms, $\lambda = 50$ s^{-1}, $5 \cdot 10^5$ triggerings in Monte-Carlo method; *right* – LIF neuron with delayed feedback for $C = 20$ mV, τ_M = 3 ms, $\Delta = 18$ ms, $y_0 = 15$ mV, $\lambda = 75$ s^{-1}, $5 \cdot 10^5$ triggerings in Monte-Carlo method.

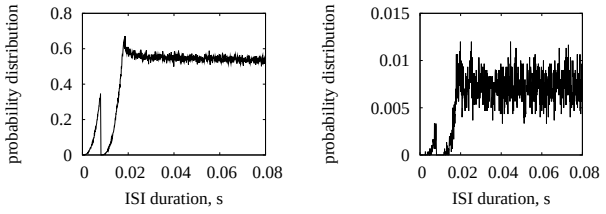

Fig. 8. ISI probability density $P^{\Delta}(t)$ (measured in s^{-1}) found numerically for τ = 10 ms, $\Delta = 8$ ms, λ = 50 s^{-1}. *Left* — $N_0 = 4$, *right* — $N_0 = 6$. In both cases $3 \cdot 10^7$ triggerings were taken.

where

$$B_1 = 3\,e^{-4\lambda\Delta} - 8\,e^{-3\lambda\Delta} + 2(6\lambda\Delta + 13)\,e^{-2\lambda\Delta} - \\ - 8(2\lambda\Delta + 3)\,e^{-\lambda\Delta} + 12\lambda^2\Delta^2 + 52\lambda\Delta + 51,$$

$$B_2 = -2\,e^{-4\lambda\Delta} + 4\,e^{-3\lambda\Delta} + 2(-5\lambda\Delta + \lambda\tau - 7)\,e^{-2\lambda\Delta} + \\ + 4(2\lambda\Delta + 3)\,e^{-\lambda\Delta} - 12\lambda^2\Delta^2 + 4\lambda^2\Delta\tau - 34\lambda\Delta + 6\lambda\tau - 24,$$

$$B_3 = e^{-4\lambda\Delta} + 2(4\lambda\Delta + 3)\,e^{-2\lambda\Delta} + 12\lambda^2\Delta^2 + 24\lambda\Delta + 9. \qquad (33)$$

It is clear, that for $\Delta = 0$ Eqs. (32), (33) must give the output ISI coefficient of variation of BN without feedback, c_v^0. And indeed, substituting $\Delta = 0$ to (32) and (33), one obtains

$$\left(c_v^{\Delta}\right)^2\Big|_{\Delta=0} = \frac{1}{(2e^{\lambda\tau} - 1)^2} \cdot \left(2\,e^{2\lambda\tau} + 2(\lambda\tau - 1)\,e^{\lambda\tau} + 1\right) = \left(c_v^0\right)^2,$$

where c_v^0 was previously found in [19].

7 Numerical Simulations

We have also performed numerical simulations of inhibitory BN with delayed feedback. A C++ program developed is similar to that used for excitatory BN with delayed feedback[20]. The class of objects, which reproduce the operation manner of inhibitory BN with delayed feedback, was created. Object of this class receives the sequence of pseudorandom numbers with Poisson distribution to its input, which is realized using tools from the GNU Scientific Library[1].

BN firing statistics is represented in terms of $P^{\Delta}(t)$, $f(s)$, λ_o^{Δ} and c_v^{Δ}. Numerical results obtained are then compared with corresponding analytical expressions, given in Eqs. (20), (23) – (27), (16) – (18), (30), (32) and (33). It was found, that numerically obtained curves fit perfectly with mentioned analytical expressions, see example in Fig. 3.

Also the set of numerical simulations for BN with higher threshold as well as for the case $\Delta \geq \tau$ was performed. All the ISI probability densities found are similar to those obtained analytically for threshold 2 and $\Delta < \tau$, see Figs. 7, left and 8.

In order to omit the model limitations and to figure out, what pequliarities of the ISI probability density are caused namely by the presence of delayed feedback, we have also performed numerical simulations of an inhibitory leaky integrate-and-fire (LIF) neuron with delayed feedback. Namely, the LIF neuron is characterized by a threshold, C, and every excitatory input impulse advances by y_0 the LIF membrane voltage, V. Between input impulses, V decays exponentially with time constant τ_M. The LIF neuron fires when V becomes greater or equal C, and $V = 0$ just after firing. When the inhibitory impulse arrives, it resets neuron's membrane potential to zero. The LIF model doesn't allow exact mathematical treatment due to gradual exponential decay of input impulses.

Thus, the program developed was extended with the class of objects, which mimics the operation manner of inhibitory LIF neuron with delayed feedback. The objects of this class are fed externally with the same sequence of pseudorandom numbers (input ISIs) as the objects of the class, based on the BN model. It was found for several parameter sets, that obtained ISI distribution for LIF model is qualitatively similar to what was found for the BN model, see example in Fig. 7, right.

8 Discussion and Conclusions

We investigated here the firing statistics of a single inhibitory neuron with delayed feedback under Poisson stimulation. Using binding neuron model, we calculate analytically the output ISI probability density, as well as the mean output ISI and the coefficient of variation for the threshold 2. For higher thresholds, mentioned statistical properties are found numerically by means of Monte-Carlo simulations.

In order to elucidate whether the features of neuronal firing statistics found are due to the the BN neuron model specifics, or namely due to the delayed feedback presence, the numerical simulations of a single inhibitory leaky integrate-and-fire neuron with delayed feedback were also performed. The LIF neuron was driven externally with the Poisson stream, which is the same as for BN.

The ISI probability densities found both for inhibitory BN and inhibitory LIF neuron exhibit several qualitatively similar pequliarities. Namely, for all the parameters sets, the $P^{\Delta}(t)$ are found to be bimodal functions, which contain jumps and derivative discontinuities, see Figs. 3, 7 and 8.

[1] http://www.gnu.org/software/gsl/

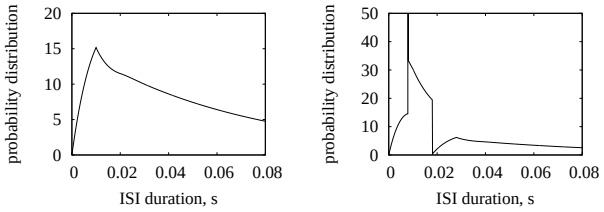

Fig. 9. ISI probability density $P^{\Delta}(t)$, s^{-1}. *Left* – BN without feedback [18]; *right* – for excitatory neuron BN with delayed feedback [20]. In both cases, τ = 10 ms, λ = 50 s^{-1}, $N_0 = 2$. For right pannel, $\Delta = 8$ ms.

Break, or jump, in ISI probability density at $t = \Delta$ is caused by the assumption of fixed time delay Δ of the impulse in the feedback line. Breaks of the same nature were observed before both for excitatory BN and excitatory LIF neuron with instantaneous [19] and delayed feedback [20].

The derivative discontinuities in ISI probability density are due to the time decay of the traces of inputs in neuron's memory, which is true both for BN and for LIF models. Such derivative discontinuinies were found in the case of no feedback, and also both for excitatory neuron with instantaneous and for excitatory neuron with delayed feedback.

In order to get visual impression of how does the delayed feedback presence reshape neuron's firing statistics of inhibitory neuron as compared to the case without feedback, we have placed here the typical output ISI probability density for BN without feedback, see Fig. 9, left. The exact expressions for this probability density are given in Eq. (1).

In the absence of feedback, bimodality and breaks in ISI probability density are not observed, see Fig. 9, left. One can conclude, that it is namely the delayed feedback presence, which causes transformation of continuous and unimodal output ISI probability density to the bimodal function with jump.

In Fig. 9, right, the tipycal output ISI probability density for excitatory BN with delayed feedback is placed, see [20] for details. In the case of excitatory neuron with delayed feedback, the output ISI probability density is multimodal function, which contains singularity of Dirac δ-function type at $t = \Delta$, exhibits jumps and derivative discontinuities. Due to the absence of δ-shaped peak, the observed number of jumps and modes, the ISI probability density for inhibitory BN with delayed feedback can be easily distinguished from the ISI probability density for excitatory BN with delayed feedback.

Also, we calculated here the mean output intensity, or firing rate, which is inverse mean output ISI. For inhibitory neuron, the output firing rate was reduced by the delayed feedback, as expected, see Fig. 4, left. For higher thresholds, the range of input intensities, at which the output firing is almost improbable, becomes wider, see Fig. 4, right. In other words, the higher threshold is the stronger stimulation is needed to evoke response. The obtained input-output relationship for BN firing intensities resembles those found experimentally for real neurons under natural stimulation[5, Fig. 4]. In contrast to the case of feed-forward shunting inhibition[4], the delayed feedback presence was not found to change the sigmoid input-output relationship qualitatively.

As regards the output ISI coefficient of variation, the considerable variability of output ISIs was found both for inhibitory BN and inhibitory LIF neuron with delayed feedback. CV was found as the function ranging between 0.5 and 1, see Figs. 5 and 6. This is consistent with experimental results [7, 13], where high CV values of the same range were obtained at the output of cortical neurons.

From Fig. 6 one can see, that delayed feedback influences CV for both BN and LIF neuron in a similar manner. In contrast to the case of excitatory neuron with delayed feedback, the delayed feedback presence does not change CV values of inhibitory neuron substantially as compared to the case without feedback. This is in accordance with experimental studies of the influence of independent GABA-mediated inhibition on * CV value of cortical neurons[5, 14].

We conclude, that the output firing statistics of an inhibitory neuron undergoes substantial changes due to the action of delayed feedback. These changes are qualitatively distinct from those, imposed by the delayed feedback on excitatory neuron.

References

1. V. Aroniadou-Anderjaska, M. Ennis and M.T. Shipley, Dendrodendritic recurrent excitation in mitral cells of the rat olfactory bulb, J. Neurophysiol. **82**, (1999) pp. 489–494.
2. A. Bacci, J.R. Huguenard and D.A. Prince, Functional autaptic neurotransmission in fast-spiking interneurons: A novel form of feedback inhibition in the neocortex, J. Neurosci. **23**, 3, (2003) pp. 859–866.
3. A. Bacci, J.R. Huguenard and D.A. Prince, Long-lasting self-inhibition of neocortical interneurons mediated by endocannabinoids, Nature **431**, (2004) pp. 312–316.
4. M. Ferrantea, M. Miglioreb and G.A. Ascolia, Feed-forward inhibition as a buffer of the neuronal input-output relation, PNAS * **106**, 42, (2009) pp. 18004–18009.
5. A. Harsch and H.P.C. Robinson, Postsynaptic Variability of Firing in Rat Cortical Neurons: The Roles of Input Synchronization and Synaptic NMDA Receptor Conductance, J. Neurosci. **20**, 16, (2000) pp. 6181–6192.
6. D.M. MacKay, Self-organization in the time domain, in *Self-Organizing Systems*, edited by M.C. Yovitts, G.T. Jacobi and G.D. Goldstein (Spartan Books, Washington, 1962), pp. 37–48.
7. M.P. Nawrot, C. Boucsein, V. Rodriguez-Molina, A. Aertsen, S. Grün and S. Rotter, Serial interval statistics of spontaneous activity in cortical neurons in vivo and in vitro, Neurocomputing **70**, (2007) pp. 1717–1722.
8. R.A. Nicoll and C.E. Jahr, Self-excitation of olfactory bulb neurones, Nature **296**, (1982) pp. 441–444.
9. T.W. Margrie, B. Sakmann and N.N. Urban, Action potential propagation in mitral cell lateral dendrites is decremental and controls recurrent and lateral inhibition in the mammalian olfactory bulb, PNAS **98**, 1, (2001) pp. 319–324.
10. J.P. Segundo, G.P. Moore, L.J. Stensaas and T.H. Bullock, Sensitivity of neurons in Aplysia to temporal pattern of arriving impulses, J.exp.Biol. **40**, (1963) pp. 643–667.
11. J.P. Segundo, D. Perkel, H. Wyman, H. Hegstad and G.P. Moore, Input-output relations in computer-simulated nerve cell, Kybernetic **4**, (1968) pp. 157–171.
12. T.C. Smith and C.E. Jahr, Self-inhibition of olfactory bulb neurons, Nature Neuroscience **5**, 8, (2002) pp. 760–766.

13. W.R. Softky and C. Koch, The highly irregular firing of cortical cells is inconsistent with temporal integration of random EPSPs, J. Neurosci. **13**, (1993) pp. 334–350.
14. C.F. Stevens, A.M. Zador, Input synchrony and the irregular firing of cortical neurons, Nat. Neurosci. **1**, (1998) pp. 210–217.
15. A.K. Vidybida, Neuron as time coherence discriminator, Biol. Cybern. **74**, (1996) pp. 539–544.
16. A.K. Vidybida, Inhibition as binding controller at the single neuron level, BioSystems **48**, (1998) pp. 263–267.
17. A.K. Vidybida, *Stochastic Models* (ISBN 966-02-3882-7, 2006).
18. A.K. Vidybida, Output stream of a Binding Neuron, Ukrainian Mathematical Journal **50**, 12, (2007) pp. 1819–1839.
19. A.K. Vidybida, Output stream of Binding Neuron with instantaneous feedback, Eur. Phys. J. B **65**, 4, (2008) pp. 577–584; Eur. Phys. J. B **69**, 2, (2009) p. 313.
20. A.K. Vidybida, K.G. Kravchuk, Output stream of Binding Neuron with delayed feedback, Eur. Phys. J. B **72**, (2009) pp. 279–287.